IEEE Access
Multidisciplinary | Rapid Review | Open Access Journal

Received January 27, 2019, accepted February 10, 2019, date of publication February 19, 2019, date of current version March 8, 2019.

Digital Object Identifier 10.1109/ACCESS.2019.2900248

A Compact LTCC Decoupling-Network Based on Coupled-Resonator for Antenna Interference Suppression of Adjacent Frequency Bands

KE-WEI QIAN
RIEST, University of Electronic Science and Technology of China, Chengdu 610054, China
Corresponding author: Ke-Wei Qian (qiankewei@uestc.edu.cn)

ABSTRACT A low-temperature co-fired ceramic (LTCC) coupled resonator decoupling network (CRDN) with asymmetric input/output (I/O) couplings for suppressing interference between two adjacent frequency bands is proposed in this paper. Based on LTCC multilayer technology, a second-order CRDN module is realized by strongly coupled semi-lumped *LC* resonators in a very small volume of 3.2 mm × 2.5 mm × 1.2 mm. A wide range of mutual admittance and different self-admittances of the CRDN can be realized by adjusting the asymmetric I/O couplings. Thus, a satisfactory decoupling performance covering two contiguous bands, as well as good matching in each band, can be realized without additional matching networks. To prove the concept, two planar inverted-F antennas working in TD-LTE and Wi-Fi frequency bands, along with the corresponding decoupling network, are designed, fabricated, and tested. The measured results have demonstrated that more than 15-dB isolation improvement can be achieved within the two operating bands, showing the feasibility of this ''one-fit-all'' integrated solution. More importantly, the design methodology and circuit topology presented in this paper are general and can be applied to practical multi-input multi-output system applications.

INDEX TERMS LTCC, decoupling network, coupled resonator, MIMO.

I. INTRODUCTION

In order to satisfy the demands of various wireless services in today's communication systems, more and more antennas of different operating frequency bands are integrated into one increasingly miniaturized physical device. Accordingly, the spatial isolation between antennas becomes more and more insufficient, which causes severe radio interferences among collocated systems. In fact, such coexistence interferences impact almost all modern wireless communication devices, like radio units of base stations and mobile terminals. Take a mobile phone or a tablet for instance, various communication protocols, including 2G (GSM), 3G (UMTS), 4G (LTE), Wi-Fi, GPS and Bluetooth, coexist in a very compact space, and the operating bands of which are very close to each other. Thus the mutual coupling and spatial correlation between antennas are severe, leading to a low radiation efficiency. Even worse, when mutual coupling is strong, the power will be coupled from one antenna to others rather than radiating to free space, which in turn decreases signal-to-noise ratio and channel capacity. These effects will eventually deteriorate the performance of the collocated systems which operate at the same or adjacent frequency bands [1]. Therefore, effectively mitigating the mutual coupling of collocated antennas and suppressing the interference of coexisted systems have become top technological challenge in electronic and communication system design [2]–[5], as the size of wireless device continuously decreases and the number of services increases. In [6] and [7], two bandpass and bandstop filters, whose design methodology and implementation are very mature, are used for interference suppression. However, for collocated systems with same or contiguous frequency bands, as shown in Figure 1, it is almost impossible to realize high isolation between them by traditional filter topology, since the limitation of selectivity cannot be easily transcended.

Some solutions for reducing mutual coupling of multi-input multi-output (MIMO) systems have been reported in recent years. Orthogonal radiation modes of highly coupled arrays are utilized as independent information channels to avoid mutual coupling and interference [8]. This mode-based array is very compact without suffering undesired effects

The associate editor coordinating the review of this manuscript and approving it for publication was Yingsong Li.

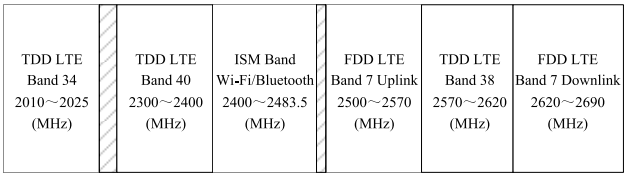

FIGURE 1. Commonly used frequency bands for mobile communication over 2000 MHz to 3000 MHz.

such as impedance mismatch or pattern distortion. A simple reactive element decoupling network is proposed in [9]. Good isolation is realized while the decoupling bandwidth is relative narrow, due to the fact that the unwanted mutual coupling is canceled only at a single frequency theoretically. Moreover, since the zero of a shunt reactive element locates either at $\omega = 0$ or $\omega = \infty$, which is far away from the resonant frequency of the antennas, it is required two additional matching networks for impedance matching. In [10]–[12], a new technique named Coupled Resonator Decoupling Network (CRDN) is proposed for decoupling two and three strongly coupled antennas. The basic principle is to design a second order coupled resonator network whose mutual admittance is opposite to that of the coupled antennas. Thus the unwanted mutual coupling of the antennas can be canceled in a relatively wide frequency band by connecting the CRDN to coupled array in shunt. Besides, some other techniques like electromagnetic band gap (EBG) [13]–[15], defected ground structure (DGS) [16], [17], neutralization line (NL) [18] and parasitic scatter [19] are also effective solutions to realize good isolation between coexisted antennas. However, none of them works for two antennas operating in two adjacent frequency bands.

In order to achieve good interference suppression between two strongly coupled antennas in complex electromagnetic environment of portable mobile terminals, a small footprint surface mountable device which is independent to the form factors of the antennas would be highly desirable. In this paper, an integrated CRDN for two coupled antennas of arbitrary form factors is proposed. The CRDN is composed of two parts: (a) a multilayered low temperature co-fired ceramic (LTCC) module that consists of two tightly coupled semi-lumped resonators; (b) two adjustable asymmetric I/O couplings, which allows the LTCC module to be adopted for different antenna form factors. Therefore, different from other existing diplexer or decoupling solutions, good decoupling and matching can be simultaneously achieved over two adjacent or contiguous frequency bands by the proposed compact decoupling network without additional matching circuit, which is very suitable for interference suppression of collocated systems in modern mobile terminals. Furthermore, the frequency bands outside the decoupled bands will not be affected by the device due to the transmission zero of filter-like feature of the LTCC device.

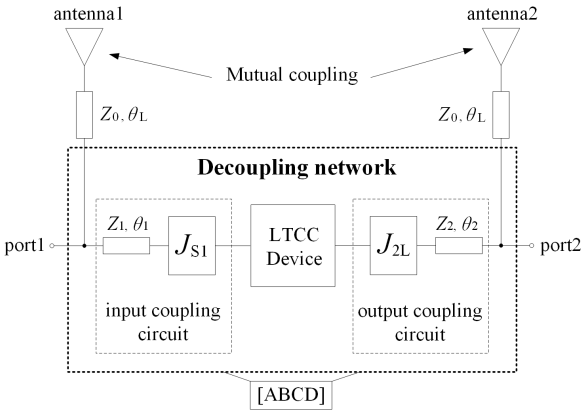

FIGURE 2. Network representation of two coupled antennas in shunt with the proposed CRDN.

II. THEORY AND DESIGN

A. DERIVATION OF DECOUPLING AND MATCHING CONDITIONS

To ease the illustration, two coupled antennas are represented by a 2×2 admittance matrix with complex entries. The CRDN consisting of one consolidated LTCC module and two adjustable I/O couplings is connected in shunt to the coupled antennas, as shown in Figure 2. Therefore, the admittance of the connected network is the sum of the two individual admittance matrices:

$$Y = \begin{bmatrix} Y_{11} & Y_{12} \\ Y_{21} & Y_{22} \end{bmatrix} = \begin{bmatrix} Y_{11}^A + Y_{11}^N & Y_{12}^A + Y_{12}^N \\ Y_{21}^A + Y_{21}^N & Y_{22}^A + Y_{22}^N \end{bmatrix} \quad (1)$$

where Y^A and Y^N represent the admittance matrix of the coupled antennas working at adjacent/contiguous frequency bands and the related decoupling network, respectively. Apparently, good isolation between the two ports of the entire network could be achieved within a given frequency range if:

$$Y_{21}(\omega_r) = Y_{21}^A(\omega_r) + Y_{21}^N(\omega_r) \approx 0 \quad (2)$$

where ω_r is the radian frequency variable.

It should be noted that if the sum of Y_{21}^A and Y_{21}^N could approach zero over two adjacent bands, high interference suppression between the two systems could be achieved. Since the designed CRDN is assumed to be lossless, the entries of the admittance matrix Y^N are all purely imaginary, while the entries of Y^A are complex in general. Thus the decoupling condition can be simplified as:

$$\mathrm{Re}\{Y_{21}^A(\omega_0)\} \approx 0 \quad (3a)$$

$$\mathrm{Im}\{Y_{21}^A(\omega_0)\} + \mathrm{Im}\{Y_{21}^N(\omega_0)\} \approx 0 \quad (3b)$$

$$\omega_0 = \sqrt{\omega_1 \cdot \omega_2} \quad (3c)$$

where ω_1 and ω_2 are the central points of the two adjacent frequency bands, respectively. Assuming that the coupled antennas separately resonant at ω_1 and ω_2, and both of them are also well matched at ω_0, then equation (3a) can be realized by introducing a piece of transmission line of electrical length

θ_L and characteristic impedance Z_0 at each antenna port. Supposing the coupling coefficient of the original antenna array is expressed as $|S_{21}|\, e^{j\phi_{21}}$ in general, θ_L can be calculated by [7]:

$$\theta_L = \frac{1}{2}\left[\phi_{21} \pm (k\pi - \frac{\pi}{2})\right], \quad k = 1, 2, 3\cdots \tag{4}$$

Similarly, when the decoupling condition is satisfied, which means $S_{21} \approx 0$ over the two adjacent bands, the matching condition can be expressed as:

$$\mathrm{Re}\{Y_{ii}^{A}(\omega_i)\} = Y_0, \quad i = 1, 2 \tag{5a}$$

$$\mathrm{Im}\{Y_{ii}^{A}(\omega_i)\} + \mathrm{Im}\{Y_{ii}^{N}(\omega_i)\} = 0, \quad i = 1, 2 \tag{5b}$$

Since the antennas are assumed to be matched at ω_1 and ω_2, respectively, equation (5b) can be simplified to:

$$\mathrm{Im}\{Y_{11}^{N}(\omega_1)\} = 0, \quad \mathrm{Im}\{Y_{22}^{N}(\omega_2)\} = 0 \tag{6}$$

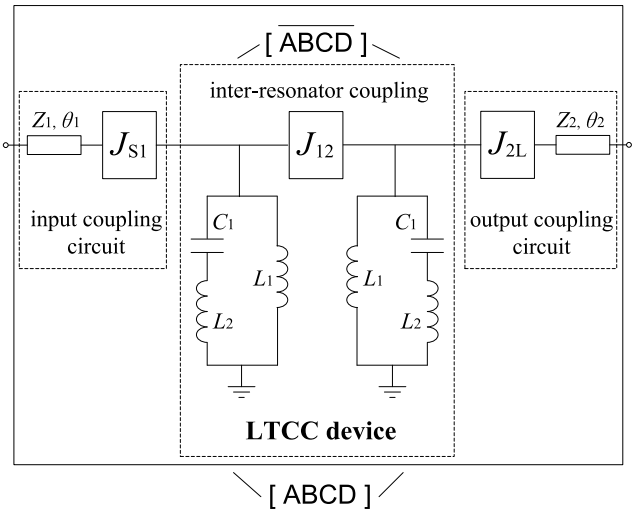

FIGURE 3. Architecture of an integrated CRDN scheme.

B. THE NETWORK REPRESENTATION

The schematic circuit of the decoupling network is depicted in Figure 3, where a second-order coupled resonator filter topology is adopted. Besides, the inter-resonator coupling and the I/O couplings are represented by admittance inverters, which are defined in the low pass domain with reference to unit termination [20]. For simplicity, it is assumed that $Z_1 = Z_2 = Z_0 = 50\Omega$. Denoting the $[ABCD]$ matrix of the LTCC module by $[\overline{ABCD}]$, which can be expressed as:

$$\overline{\mathrm{A}} = \overline{\mathrm{D}} = \frac{1 - \omega^2 C_1(L_1 + L_2)}{\omega L_1 J_{12}(\omega^2 L_2 C_1 - 1)} \tag{7a}$$

$$\overline{\mathrm{B}} = \frac{1}{jJ_{12}} \tag{7b}$$

$$\overline{\mathrm{C}} = j\frac{[1 - \omega^2 C_1(L_1 + L_2)]^2}{\omega^2 L_1^2 J_{12}(\omega^2 L_2 C_1 - 1)^2} - jJ_{12} \tag{7c}$$

Having had the $[ABCD]$ matrix of the LTCC module left- and right- cascaded with those of the input and the output coupling circuits, one can find the overall $[ABCD]$ matrix of the decoupling network, from which the Y parameters of the decoupling network can be found as:

$$Y_{11}^{N} = \frac{D}{B}, \quad Y_{22}^{N} = \frac{A}{B} \tag{8a}$$

$$Y_{21}^{N} = \frac{-1}{B} \tag{8b}$$

where A, B and D are given by the equations below:

$$\begin{aligned}\mathrm{A} = {} & \overline{\mathrm{A}}\frac{J_{S1}}{J_{2L}}\sin\theta_1\sin\theta_2 - j\overline{\mathrm{B}}Z_0 J_{S1}J_{2L}\sin\theta_1\cos\theta_2 \\ & - j\overline{\mathrm{C}}\frac{Y_0\cos\theta_1\sin\theta_2}{J_{S1}J_{2L}} - \overline{\mathrm{D}}\frac{J_{S1}}{J_{2L}}\cos\theta_1\cos\theta_2\end{aligned} \tag{9a}$$

$$\begin{aligned}\mathrm{B} = {} & -j\overline{\mathrm{A}}\frac{J_{S1}}{J_{2L}}Z_0\sin\theta_1\cos\theta_2 + \overline{\mathrm{B}}Z_0^2 J_{S1}J_{2L}\sin\theta_1\sin\theta_2 \\ & - \overline{\mathrm{C}}\frac{\cos\theta_1\cos\theta_2}{J_{S1}J_{2L}} - j\overline{\mathrm{D}}\frac{J_{S1}}{J_{2L}}Z_0\cos\theta_1\sin\theta_2\end{aligned} \tag{9b}$$

$$\begin{aligned}\mathrm{D} = {} & -\overline{\mathrm{A}}\frac{J_{S1}}{J_{2L}}\cos\theta_1\cos\theta_2 - j\overline{\mathrm{B}}Z_0 J_{S1}J_{2L}\cos\theta_1\sin\theta_2 \\ & - j\overline{\mathrm{C}}\frac{Y_0\sin\theta_1\cos\theta_2}{J_{S1}J_{2L}} + \overline{\mathrm{D}}\frac{J_{2L}}{J_{S1}}\sin\theta_1\sin\theta_2\end{aligned} \tag{9c}$$

The decoupling and matching conditions can be specified by substituting equation (8) into equations (3) and (6) for obtaining proper values of θ_1, θ_2, J_{S1}, J_{12}, J_{2L}, C_1, L_1 and L_2. Specifically, parameters C_1, L_1 and L_2 determine the working frequency of the decoupling network; the inter-resonator coupling is controlled by J_{12}; while θ_1, θ_2, J_{S1} and J_{2L} are crucial and are to be adjusted for different input/output couplings.

C. SELF-ADMITTANCE AND MUTUAL-ADMITTANCE ANALYSIS

From equations (8) and (9), it is shown that admittance parameters of the decoupling network depend on the values of θ_1, θ_2, J_{S1} and J_{2L} while the $[\overline{ABCD}]$ matrix remains unchanged. In other words, different self-admittances and mutual admittances of a CRDN can be achieved by tuning I/O couplings when the LTCC module is fixed for a given frequency band. For instance, the simulated imaginary part of Y_{11}^{N} and Y_{22}^{N} for a CRDN working over two adjacent bands with different combinations of θ_1 and θ_2 is presented in Figure 4(a). It can be seen that when $L_1 = 0.5$ nH, $L_2 = 0.3$ nH, $C_1 = 4.9$ pF, $J_{S1} = 1.05$, $J_{2L} = 0.95$ and $J_{12} = 3$ are fixed, different combinations of Y_{11}^{N} and Y_{22}^{N} can be obtained by adjusting θ_1 and θ_2 (θ_1 and θ_2 are defined at $f_0 = 2.4$ GHz). The following cases can be observed from the figure:

(a) when $\theta_1 = 20°$ and $\theta_2 = 0°$, the zeroes of $\mathrm{Im}\{Y_{11}^{N}\}$ and $\mathrm{Im}\{Y_{22}^{N}\}$ separately locate at 2.3 GHz and 2.5 GHz;
(b) when $\theta_1 = 15°$ and $\theta_2 = 2°$, the zeroes of those are 2.33 GHz and 2.46 GHz respectively;
(c) when $\theta_1 = 12°$ and $\theta_2 = 4°$, the zeroes locate at 2.36 GHz and 2.43 GHz respectively;
(d) when $\theta_1 = 8°$ and $\theta_2 = 6°$, the zeroes both locate at $f_0 = 2.4$ GHz, which means the proposed topology can also be used for symmetric antenna pair.

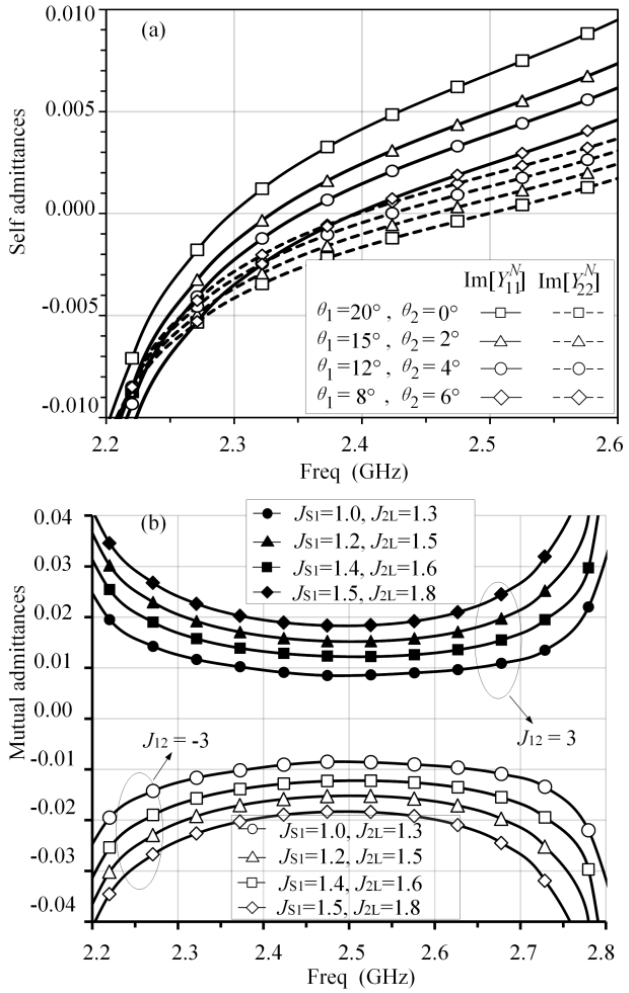

FIGURE 4. (a) Simulated self-admittances with different combinations of θ_1 and θ_2. (b) Simulated mutual-admittances against various combinations of J_{S1}, J_{2L} and J_{12}.

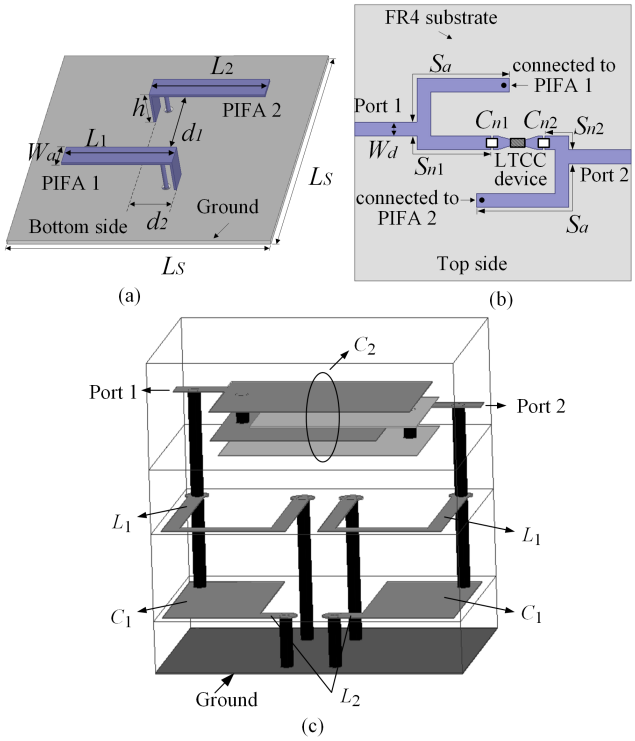

FIGURE 5. Configurations of (a) the 2.35 GHz and 2.45 GHz testing PIFA array on the front side; (b) the corresponding LTCC CRDN circuit on the back side; (c) the layout of the LTCC device.

It should be mentioned that in all the four cases, mutual admittances of the decoupling network remain almost unchanged. Namely, good isolation could be achieved for coupled antennas which resonant at different combinations of ω_1 and ω_2 according to equations (3) and (6). More importantly, since the zeroes of the self-admittances of CRDN could be adjusted by various I/O couplings, good matching can be realized without any additional matching network.

Furthermore, different mutual admittances of the presented CRDN can also be obtained by tuning I/O couplings with a fixed LTCC module, as shown in Figure 4(b). In all the cases, $L_1 = 0.5$ nH, $L_2 = 0.3$ nH, $C_1 = 4.9$ pF, $\theta_1 = \theta_2 = 7°$ and $J_{12} = \pm 3$ are fixed, while J_{S1} and J_{2L} change from 1.0 to 1.5 and 1.3 to 1.8, respectively. It can be seen that when $J_{12} = 3$, different levels of Im$\{Y_{21}^N\}$ (from 0.009 to 0.018) can be achieved by tuning J_{S1} and J_{2L} for various types of commonly used antenna pairs whose Im$\{Y_{21}^A\}$ range is from -0.009 to -0.018. Besides, coupled antennas with positive Im$\{Y_{21}^A\}$ can also be decoupled by this network topology whose corresponding negative Im$\{Y_{21}^N\}$ is realized by changing the capacitive inner coupling to inductive one, i.e., $J_{12} = -3$ in this case, as shown in Figure 4(b). This feature further justifies that the proposed decoupling network can provide a "one-fit-all" solution for a wide range of coupled antenna types with various couplings and resonant frequencies.

III. SIMULATED AND MEASURED RESULTS

To illustrate the proposed theory and topology, two examples concerning different antenna coupling mechanisms are presented; one for coupled planar inverted-F antenna (PIFA) array while the other one for practical collocated Flexible Printed Circuit (FPC) antennas in mobile phones. In both cases, an LTCC device with relative dielectric constant of 9.2 and loss tangent of 0.002 at the frequency of interest is utilized. It consists of two semi-lumped element resonators and one coupling capacitor. With an 8-layer vertical structure, the LTCC device has a compact volume of $3.2\times2.5\times1.2$ mm^3. Full-wave EM simulation is performed using Agilent EMPro [21].

A. AN LTCC CRDN FOR A PIFA ARRAY

Two PIFAs working at 2.35 GHz (TDD LTE band 40) and 2.45 GHz (ISM band) respectively and the corresponding LTCC decoupling network are given in this section. The

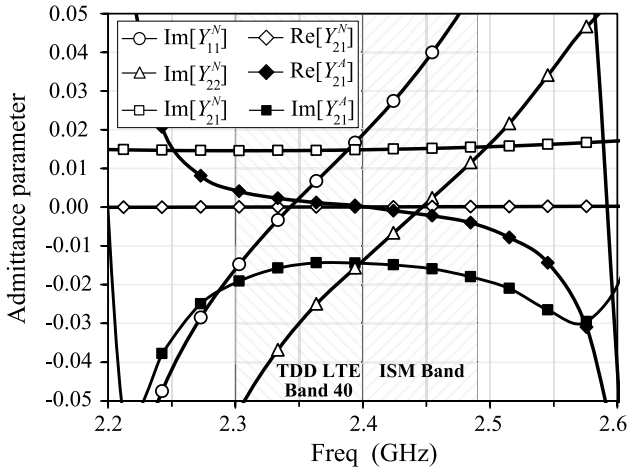

FIGURE 6. Tested admittance parameters of the PIFA array and the decoupling network.

configuration of the entire network and detailed structure of the LTCC device are illustrated in Figure 5. It can be seen that the two PIFAs and the LTCC CRDN, which are connected by two posts, are mounted on each side of a 60 mm $\times$ 60 mm FR4 substrate. As shown in Figure 5(a), the two antennas are coupled at a distance of $d_1 = 17$ mm in the X-direction and $d_2 = 10$ mm in the Y-direction, while the other antenna relevant dimensions are $L_1 = 26$ mm, $L_2 = 25$ mm, $h = 6.3$ mm and $W_a = 5$ mm. Figure 5 (b) shows the corresponding decoupling network, a section of transmission line of length S_a and characteristic impedance of Z_0 is inserted at each antenna port to realize $\mathrm{Re}\{Y_{21}^A\} = 0$ according to equation (4). Here, since the coupled PIFA array has a mutual admittance of -0.015j around $f_0 = 2.4$ GHz as shown in Figure 6, the Y_{21}^N is designed to be 0.015j to cancel the Y_{21}^A over the two contiguous frequency bands according to equation (3), and J_{S1}, J_{2L} and J_{12} are all implemented by capacitive couplings in this case. Meanwhile, the zeroes of $\mathrm{Im}\{Y_{11}^N\}$ and $\mathrm{Im}\{Y_{22}^N\}$ are designed to locate at the middle point of each frequency band respectively according to equation (6), thus no extra matching network is required after decoupling. The corresponding physical parameters of the decoupling network are: $W_d = 3$ mm, $S_a = 25.5$ mm, $S_{n1} = 15$ mm, $S_{n2} = 8$ mm, $C_{n1} = 3.9$ pF and $C_{n2} = 2.7$ pF; while the lumped-element values of the LTCC device are chosen as: $L_1 = 1.9$ nH, $L_2 = 0.5$ nH, $C_1 = 1.2$ pF and $C_2 = 4.5$ pF.

Figure 7(a)-(b) shows the simulated and measured responses of the entire decoupled network. Obviously, an improvement of at least 13 dB in isolation has been achieved after decoupling within the two contiguous frequency bands. Accordingly, the 6 dB matching bandwidths of the two PIFAs decrease from 180 MHz to 135 MHz (TDD LTE band 40) and 212 MHz to 150 MHz (ISM band), respectively. It is because for two coupled antennas, one acts as a lossy load for the other. Thus it is understandable that the matching bandwidth for a lossier antenna is wider [22]. However, despite a slightly narrower matching bandwidth, the radiation efficiencies of the decoupled antennas are greater than those of coupled ones. Figure 7(c) presents the measured efficiencies of the two

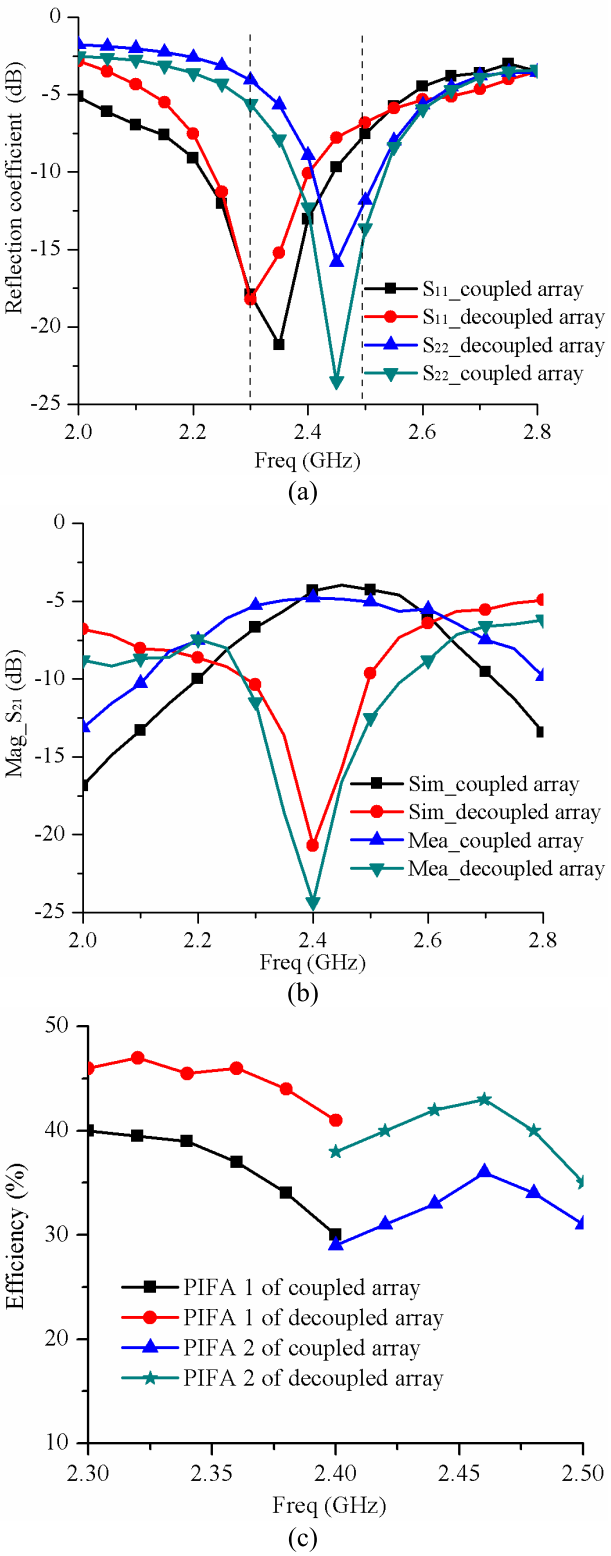

FIGURE 7. (a) Measured reflection responses of the coupled and decoupled PIFA array; (b) simulated and measured isolations of the coupled and decoupled PIFA array; (c) efficiencies of the proposed PIFAs before and after decoupling.

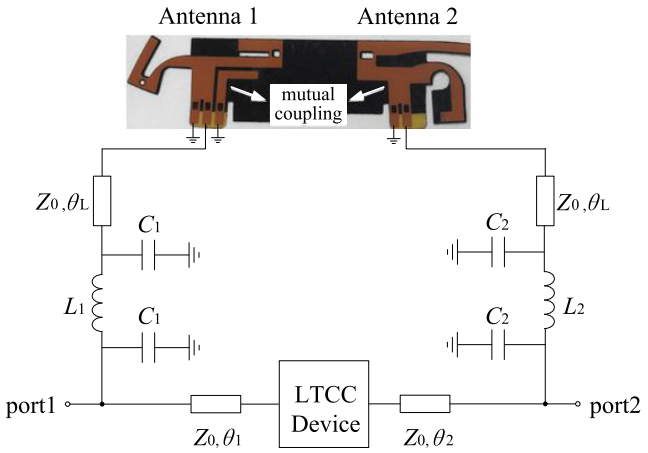

FIGURE 8. Schematic of a decoupling solution for practical mobile phone antennas with LTCC CRDN.

PIFAs before and after decoupling to further illustrate the merits of the proposed LTCC CRDN. It is seen that an obvious improvement in efficiency can be achieved when the proposed LTCC CRDN is utilized, which could be very valuable for practical applications of mobile devices.

B. AN LTCC CRDN FOR COLLOCATED MOBILE PHONE ANTENNAS

In order to further demonstrate the effectiveness of the proposed LTCC CRDN for coexisted systems, a mobile phone with two collocated antennas working at 1.9 GHz ∼ 2.5 GHz and 2.4 GHz ∼ 2.48 GHz respectively as well as the related LTCC CRDN will be discussed in this section. As shown in Figure. 8, the related decoupling network consists of one LTCC device, two "π" networks and four pieces of transmission lines. Similarly, a piece of transmission line of θ_L is inserted at each port of the antenna to realize $\mathrm{Re}\{Y_{21}^A\}= 0$, while the "$\pi$" networks are utilized not only to enhance the matching performance, but to fine tune the electrical lengths of θ_L due to the fact that frequency deviation might occur when the battery and back cover of the mobile phone are considered in practical circumstance. Here, the LTCC device is the same as the abovementioned example since the two coupled antennas resonate at the specified frequency bands as that of Figure 5(a), which further verifies its "one-fit-all" feature. Besides, the transmission lines of θ_1 and θ_2 are utilized for adjusting the value of $\mathrm{Im}\{Y_{21}^N\}$ and the zeroes of $\mathrm{Im}\{Y_{11}^N\}$ and $\mathrm{Im}\{Y_{22}^N\}$.

In this practical case, the overlapped frequency band (2.4 GHz ∼ 2.48 GHz) of the antennas, where the greatest coupling occurs, has to be decoupled. The parameters of the decoupling network are chosen as follows: $\theta_L = 7°$, $\theta_1 = 7°$, $\theta_2 = 7°$, $L_1 = 1.9$ nH, $L_2 = 0.5$ nH, $C_1 = 1.2$ pF and $C_2 = 4.5$ pF. The measured responses of the entire decoupled network are shown in Figure 9. It is seen that for the commonly accepted 6 dB return loss requirement for practical mobile terminals, the matching bandwidths of

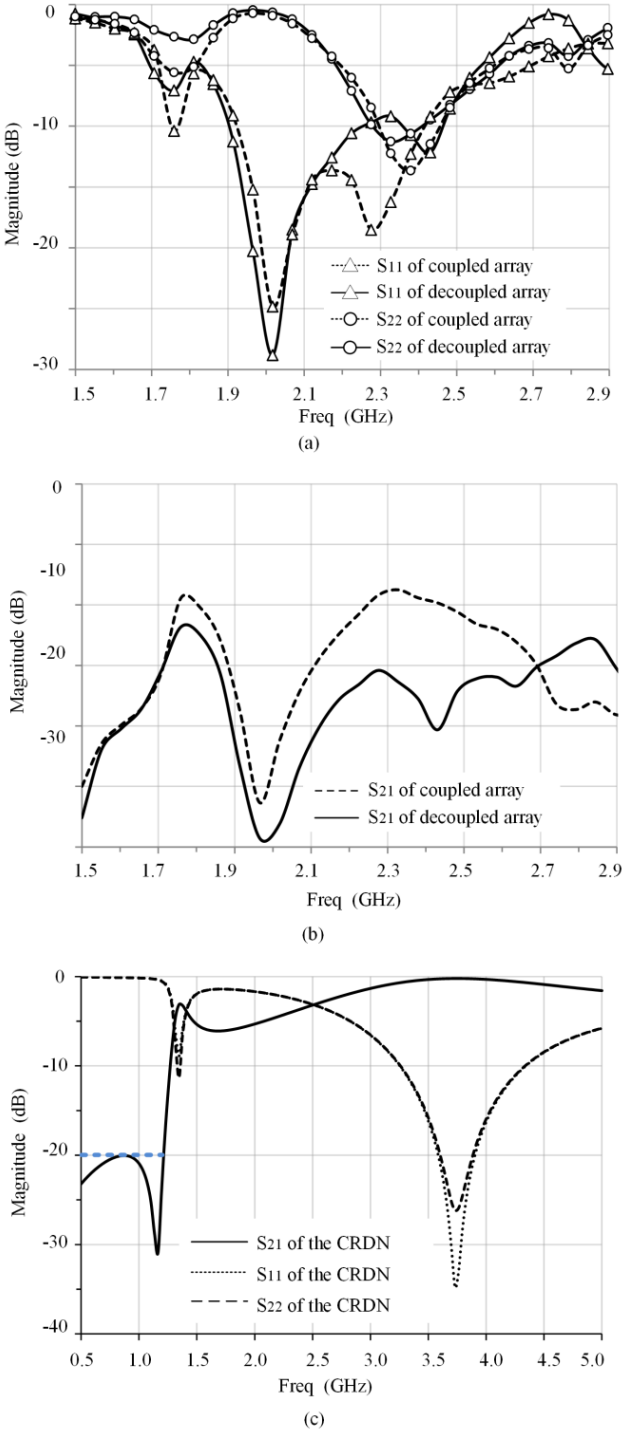

FIGURE 9. (a) Measured reflection responses of the coupled and decoupled mobile phone antenna array; (b) measured isolations of the coupled and decoupled mobile phone antenna array; (c) measured Sparameters of the CRDN.

the two collocated antennas almost remain unchanged after decoupling, while an 8 dB improvement of isolation has been achieved within the band of interest.

Besides, a transmission zero can be created in lower frequency band due to the filter-like feature of the CRDN device.

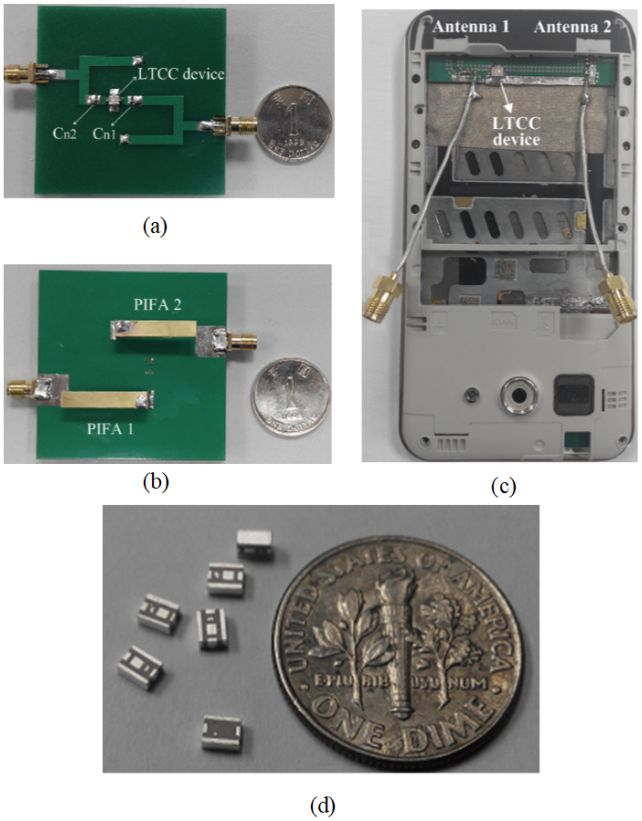

FIGURE 10. Photos of (a) back side of the testing board for PIFAs with an LTCC CRDN; (b) front side of the testing board for PIFAs; (c) testing board for practical mobile phone antennas with an LTCC CRDN; and (d) samples of the LTCC CRDN device.

As shown in Figure 9(c), the transmission coefficient S_{21} of the LTCC CRDN is below -20 dB from 0.5 GHz to 1.2 GHz, meanwhile S_{11} and S_{22} are approximately equal to 0 dB within the band. That is to say, the frequency bands outside the bands of interest, such as LTE 700, GSM 850/WCDMA 850 and GSM 900 will not be affected by the device. Obviously, it will be another attractive feature for practical applications of mobile devices. The photos of the illustrated antenna arrays along with some samples of the LTCC CRDN device are shown in Figure 10.

IV. CONCLUSION

An integrated LTCC coupled resonator decoupling network for interference suppression of coexisted antennas was proposed in this paper. With a consolidated LTCC device for a given frequency band and two adjustable I/O couplings, the proposed decoupling scheme can be applied to various antenna arrays without additional matching network. Taking the advantage of the LTCC multilayer technology, the integrated CRDN device can be made in a compact volume. Moreover, it can be designed using existing filter design theory and realization techniques due to the filter-like topology. The design theory of the proposed device and the design guidelines are also given in this paper. To demonstrate the proposed decoupling scheme, two examples of different types of antennas, including PIFAs and practical FPC antennas of a mobile phone, are given. All the coupled antenna arrays in this paper are decoupled using the same LTCC CRDN device but with different external I/O components. The simulated and measured results verify that good decoupling and matching conditions can be achieved within the band of interest. It can be foreseen that the proposed integrated CRDN device has a great potential for future wireless mobile terminals that are equipped with collocated antennas working at adjacent or contiguous frequency bands.

REFERENCES

[1] Z. Hu, R. Susitaival, Z. Chen, I-K. Fu, P. Dayal, and S. K. Baghel, "Interference avoidance for in-device coexistence in 3GPP LTE-Advanced: Challenges and solutions," *IEEE Commun. Mag.*, vol. 50, no. 11, pp. 60–67, Nov. 2012.

[2] A. Raghavan, E. Gebara, E. M. Tentzeris, and J. Laskar, "Analysis and design of an interference canceller for collocated radios," *IEEE Trans. Microw. Theory Techn.*, vol. 53, no. 11, pp. 3498–3508, Nov. 2005.

[3] J. Weber, C. Volmer, K. Blau, R. Stephan, and M. A. Hein, "Miniaturized antenna arrays using decoupling networks with realistic elements," *IEEE Trans. Microw. Theory Techn.*, vol. 54, no. 6, pp. 2733–2740, Jun. 2006.

[4] F. Liu, J. Guo, L. Zhao, X. Shen, and Y. Yin, "A meta-surface decoupling method for two linear polarized antenna array in sub-6 GHz base station applications," *IEEE Access*, vol. 7, pp. 2759–2768, 2018.

[5] K. Yu, Y. Li, and X. Liu, "Mutual coupling reduction of a MIMO antenna array using 3-D novel meta-material structures," *Appl. Comput. Electromagn. Soc. J.*, vol. 33, no. 7, pp. 758–763, 2018.

[6] H. Khatri, P. S. Gudem, and L. E. Larson, "Integrated RF interference suppression filter design using bond-wire inductors," *IEEE Trans. Microw. Theory Techn.*, vol. 56, no. 5, pp. 1024–1034, May 2008.

[7] K. Rambabu, M. Y.-W. Chia, K. M. Chan, and J. Bornemann, "Design of multiple-stopband filters for interference suppression in UWB applications," *IEEE Trans. Microw. Theory Techn.*, vol. 54, no. 8, pp. 3333–3338, Aug. 2006.

[8] L. K. Yeung and Y. E. Wang, "Mode-based beamforming arrays for miniaturized platforms," *IEEE Trans. Microw. Theory Techn.*, vol. 57, no. 1, pp. 45–52, Jan. 2009.

[9] S.-C. Chen, Y.-S. Wang, and S.-J. Chung, "A decoupling technique for increasing the port isolation between two strongly coupled antennas," *IEEE Trans. Antennas Propag.*, vol. 56, no. 12, pp. 3650–3658, Dec. 2008.

[10] L. Zhao, F. Liu, X. Shen, G. Jing, Y.-M. Cai, and Y. Li, "A high-pass antenna interference cancellation chip for mutual coupling reduction of antennas in contiguous frequency bands," *IEEE Access*, vol. 6, pp. 38097–38105, 2018.

[11] L. Zhao and K.-L. Wu, "A broadband coupled resonator decoupling network for a three-element compact array," in *IEEE MTT-S Int. Microw. Symp. Dig.*, Jun. 2013, pp. 1–3.

[12] K.-W. Qian, G.-L. Huang, J.-J. Liang, B. Qian, and T. Yuan, "An LTCC interference cancellation device for closely spaced antennas decoupling," *IEEE Access*, vol. 6, pp. 68255–68262, 2018.

[13] F. Yang and Y. Rahmat-Samii, "Microstrip antennas integrated with electromagnetic band-gap (EBG) structures: A low mutual coupling design for array applications," *IEEE Trans. Antennas Propag.*, vol. 51, no. 10, pp. 2936–2946, Oct. 2003.

[14] L. Yang, M. Fan, F. Chen, J. She, and Z. Feng, "A novel compact electromagnetic-bandgap (EBG) structure and its applications for microwave circuits," *IEEE Trans. Microw. Theory Techn.*, vol. 53, no. 1, pp. 183–190, Jan. 2005.

[15] K. Payandehjoo and R. Abhari, "Employing EBG structures in multi-antenna systems for improving isolation and diversity gain," *IEEE Antennas Wireless Propag. Lett.*, vol. 8, pp. 1162–1165, 2009.

[16] C.-Y. Chiu, C.-H. Cheng, R. D. Murch, and C. R. Rowell, "Reduction of mutual coupling between closely-packed antenna element," *IEEE Trans. Antennas Propag.*, vol. 55, no. 6, pp. 1732–1738, Jun. 2007.

[17] M. Salehi and A. Ghorbani, "Elimination of scan blindness in microstrip scanning array antennas using defected ground structure," in *Proc. 37th Eur. Microw. Conf.*, Munich, Germany, Oct. 2007, pp. 482–484.

[18] S.-W. Su, C.-T. Lee, and F.-S. Chang, "Printed MIMO-antenna system using neutralization-line technique for wireless USB-dongle applications," *IEEE Trans. Antennas Propag.*, vol. 60, no. 2, pp. 456–463, Feb. 2012.

[19] B. K. Lau and J. B. Andersen, "Simple and efficient decoupling of compact arrays with parasitic scatterers," *IEEE Trans. Antennas Propag.*, vol. 60, no. 2, pp. 464–472, Feb. 2012.
[20] J.-S. G. Hong and M. J. Lancaster, *Microstrip Filters for RF / Microwave Applications*, 2nd ed. New York, NY, USA: Wiley, 2011, ch. 3.
[21] *EMPro 3D EM Simulation Software, Version 2012.09*, Agilent Technologies, Santa Clara, CA, USA, 2012.
[22] G. Shaker, S. Safavi-Naeini, and N. Sangary, "Q-bandwidth relations for the design of coupled multi-element antennas," in *Proc. IEEE Antennas Propag. Soc. Int. Symp.*, Jun. 2009, pp. 1–4.

KE-WEI QIAN received the M.Eng. and Ph.D. degrees from the University of Electronic Science and Technology of China, Chengdu, China, in 2006 and 2012, respectively. From 2013 to 2014, he was with the Department of Electronic Engineering, The Chinese University of Hong Kong, Hong Kong, where he was involved in various low-temperature co-fired ceramic multichip-module designs and antennas for next-generation mobile communication systems. He is currently an Associate Professor with the University of Electronic Science and Technology of China. His current research interests include design and application of microwave and millimeter-wave circuits and systems.